Atmospheric Environment 67 (2013) 287–295

Contents lists available at SciVerse ScienceDirect

Atmospheric Environment

journal homepage: www.elsevier.com/locate/atmosenv

Ozone and its projection in regard to climate change

Ani Melkonyan [a,*], Patrick Wagner [b,1]

[a] University Duisburg-Essen, Campus Essen, Faculty of Biology, Applied Climatology und Landscape Ecology, Building S-A/Room 25, Schützenbahn 70, D-45127 Essen, Germany
[b] University Duisburg-Essen, Campus Essen, Faculty of Biology, Applied Climatology und Landscape Ecology, Building S-A/Room 23, Schützenbahn 70, D-45127 Essen, Germany

HIGHLIGHTS

- Ozone dependence on NO_x and temperature at industrial and rural stations.
- Prediction of number of days with ozone exceedances in terms of climate change.
- Frequency of bad ozone days increases by 135% at the industrial station.
- Frequency of bad ozone days increases by 87% at the rural station.
- Ozone forming potential is significantly higher in rural areas than in urban ones.

ARTICLE INFO

Article history:
Received 22 May 2012
Received in revised form
11 September 2012
Accepted 15 October 2012

Keywords:
Ozone production
NO_x- and VOC-limited regimes
Probability of ozone exceedances
Limit values
ARIMA model
Global climate change
North Rhine-Westphalia

ABSTRACT

In this paper, the dependence of ozone-forming potential on temperature was analysed based on data from two stations (with an industrial and rural background, respectively) in North Rhine-Westphalia, Germany, for the period of 1983–2007. After examining the interrelations between ozone, NO_x and temperature, a projection of the days with ozone exceedance (over a limit value of a daily maximum 8-h average ≥ 120 μg m^{-3} for 25 days per year averaged for 3 years) in terms of global climate change was made using probability theory and an autoregression integrated moving average (ARIMA) model. The results show that with a temperature increase of 3 K, the frequency of days when ozone exceeds its limit value will increase by 135% at the industrial station and by 87% at the rural background station.

1. Introduction

Ozone is a secondary pollutant that is not emitted but is formed by photochemical reactions, especially during weather conditions with high solar radiation. It is vitally important to consider ozone as a pollutant not only because of its dangerous effects on the respiratory system but also because of its impact on forests and agricultural crops (Mücke et al., 2009; Booker et al., 2009). Ozone is one of the main components of photochemical smog, and ozone levels are driven by chemical reactions between oxides of nitrogen (NO_x), CO, methane and other volatile organic compounds (VOCs) in the presence of sunlight and high air temperatures (Emeis et al., 1997; Sillman, 2003; Jacob and Winner, 2009).

Motor vehicle exhaust, industrial emissions, gasoline vapours and chemical solvents as well as natural sources emit NO_x and VOC to help form ozone (Sillman, 1999; Guenther et al., 2000; Derwent et al., 2007; Saito et al., 2009). Anthropogenic emissions can form ozone even far away from the emission sources. If VOC and NO_x form peroxyacetylnitrate (PAN) in the vicinity of the sources, they can be transported over long distances to remote regions during cool weather conditions and can be released in these regions to form ozone when the temperature rises due to a change of weather

Abbreviations: NRW, North Rhine-Westphalia; NO, nitric oxide; NO_2, nitrogen dioxide; O_3, ozone; LANUV, Environmental State Agency for Nature, Environment and Consumer Protection; VOC, volatile organic compounds; NMVOC, non-methane volatile organic compounds; AVOC, anthropogenic volatile organic compounds; BVOC, biogenic volatile organic compounds; WALS, Duisburg–Walsum; EGGE, Horn-Bad Meinberg Egge; IPCC, Intergovernmental Panel on Climate Change; SRES, Special Report on Emission Scenarios.

* Corresponding author. Tel.: +49 201 183 2723; fax: +49 201 183 3239.
E-mail addresses: ani.melkonyan@uni-due.de (A. Melkonyan), patrick.wagner@uni-due.de (P. Wagner).
URL: http://www.uni-due.de/klimatologie
[1] Tel.: +49 201 183 3387.

1352-2310/$ – see front matter © 2012 Elsevier Ltd. All rights reserved.
http://dx.doi.org/10.1016/j.atmosenv.2012.10.023

conditions because PAN breaks down quickly when the temperature is high (Sillman and Samson, 1995; Beine et al., 1997).

The relation between ozone and one of its main precursors, NO_x, can be simplified to only two reactions (Atkinson, 2000; Costabile and Allegrini, 2007):

$$NO + O_3 \rightarrow NO_2 + O_2 \quad (R1)$$

$$NO_2 + O_2 + h\nu \rightarrow O_3 + NO, \quad (R2)$$

where $h\nu$ is the radiation energy with a frequency ν at wavelength $\lambda < 420$ nm, and h is the Planck constant, such that the reaction (R2) can only take place in daytime. The reactions come quickly into balance (after a few minutes), and the concentrations of NO_x and O_3 do not change further.

The other important reaction partner is a VOC molecule, which reacts with an OH radical to form a peroxide radical (RO_2) (R3). Especially under the influence of solar radiation, such reactive OH radicals are present at significant concentrations (Handisides et al., 2003).

In a subsequent reaction RO_2 oxidises NO to NO_2 (R4).

$$RH + OH + O_2 \rightarrow RO_2 + H_2O \quad (R3)$$

$$RO_2 + NO \rightarrow RO + NO_2 \quad (R4)$$

In reaction (R4) NO is oxidised to NO_2 without using O_3, and together with reaction (R2) a net production of ozone takes place. Subsequently, OH and NO_2 can react with each other (R5):

$$OH + NO_2 \rightarrow HNO_3 \quad (R5)$$

In this case, OH radicals and NO_2 are consumed to form nitric acid, and therefore, these compounds are no longer available to build up ozone by the reactions (R2)–(R4). Produced in the course of reaction (R5), nitric acid is water-dissolvable and can effectively be washed out of the atmosphere.

Which of the competing reactions (R3) and (R5) takes place depends on the NO_x concentration (Monks, 2004). Especially in urban atmosphere, many reactions determine the production and loss of OH radicals and thus ozone formation or loss (Handisides et al., 2003; Monks, 2004; Sadanaga et al., 2005; Yoshino et al., 2012).

VOCs contribute in different degrees to the formation of ozone due to their different reactivities and chemical constitutions (Carter, 1994; Atkinson, 2000; Saito et al., 2009). Since because biogenic VOCs (e.g., isoprene and monoterpenes) are quite reactive and their emission is temperature-dependent, they can form a substantial amount of ozone if the temperature is high (Fuentes et al., 2000; Lee and Wang, 2006; Narumi et al., 2009). Therefore, ozone formation seems to be temperature-dependent (Sillman and Samson, 1995; Narumi et al., 2009), although many of the reactions included in the ozone formation process are photochemical reactions and thus are light-dependent rather than temperature-dependent. Another aspect that causes the indirect dependence of ozone on temperature is the strong temperature dependence of the peroxyacetylnitrate (PAN) lifetime (Sillman and Samson, 1995; Barett et al., 1998; Kuttler, 2011). Barett et al. (1998) showed that the thermal decomposition of PAN and radiation are important factors for ozone formation. The relationship between high radiation and high temperature, especially in summer months, also results in a significant correlation between ozone and temperature. Accordingly, the registered ozone concentrations were extremely high over Europe during the heat waves in July and August 2003 (Bruckmann et al., 2003a,b) and in July 2006. In August 2003, measurements at 131 stations in 27 European countries showed that the maximum hourly ozone concentrations exceeded 220 $\mu g\ m^{-3}$ (the limit values of 1-h maximum ozone are 180 and 240 $\mu g\ m^{-3}$ for information and alarm, respectively; LANUV, 2010) over central Europe, covering a large region of Germany.

An exact investigation of the recent heat waves as a 'shape of things to come' can help both scientists in evaluating future climatic impacts and decision makers in developing appropriate response strategies. For that reason, it is absolutely necessary to model ozone behaviour in response to maximum daily temperature changes in the future.

The increase of average ozone concentrations during the last two decades at both industrial- and rural background stations was the main reason to analyse ozone behaviour patterns in detail (Melkonyan, 2011). Emphasis is given to the precursors of ozone (NO and NO_2 concentrations and their ratio; VOC data are not available) and maximum daily temperature.

On this basis, the events when ozone exceeded its limit value (daily maximum 8-h average) have been analysed to determine the probabilities of their occurrences in current and future climates at the industrial- and rural background stations in the western part of Germany.

2. Research area

The research area covers North Rhine-Westphalia state, which is the largest western Federal State of Germany in terms of population and economic output. The state has nearly 18 million inhabitants (Bezirksregierung Düsseldorf, 2010), contributes approximately 22% of Germany's gross domestic product and comprises a land area of 34.083 km^2. The region is characterised by a high population and traffic density as well as a high degree of industrialisation concentrated in the Rhine-Ruhr area. The negative impact of these conditions on the natural resources has led to intensive and successful efforts aimed at improving environmental conditions (air-pollution control, water-pollution control and soil protection). Concerning the reasons for environmental pollution, the proportion of non-point sources (traffic) has meanwhile considerably gained importance compared to point sources (industry).

In this paper, two stations (shown in the map: Fig. 1) with industrial (Duisburg Walsum, further named WALS) and rural backgrounds (Horn-Bad Meinberg Egge, named EGGE) have been chosen using the criteria of the longest dataset (running from 1983 to 2007) and the availability of data on both air-pollution and meteorological parameters.

The area where the industrial station (WALS) is located has an urban character, but the character of the station itself is an industrial one due to the existence of industrial production around it. Nearby, there are coking plants and mining, steel and paper-processing factories.

Horn-Bad Meinberg Egge (EGGE) is located in the forest area near Paderborn. Road L 826 passes by 1 km to the south. An access road runs approximately 100 m away from the station. Approximately 1.5 km to the east, there is a chip-processing factory. The remaining land is rural area.

3. Data and methods

Data on both ozone and one of its precursors (NO_x) as well as meteorology (air temperature, radiation, relative humidity, precipitation and wind speed) were provided by the North Rhine-Westphalia State Agency for Nature, Environment and Consumer Protection (LANUV, NRW, Essen) for the two stations (VOC data are

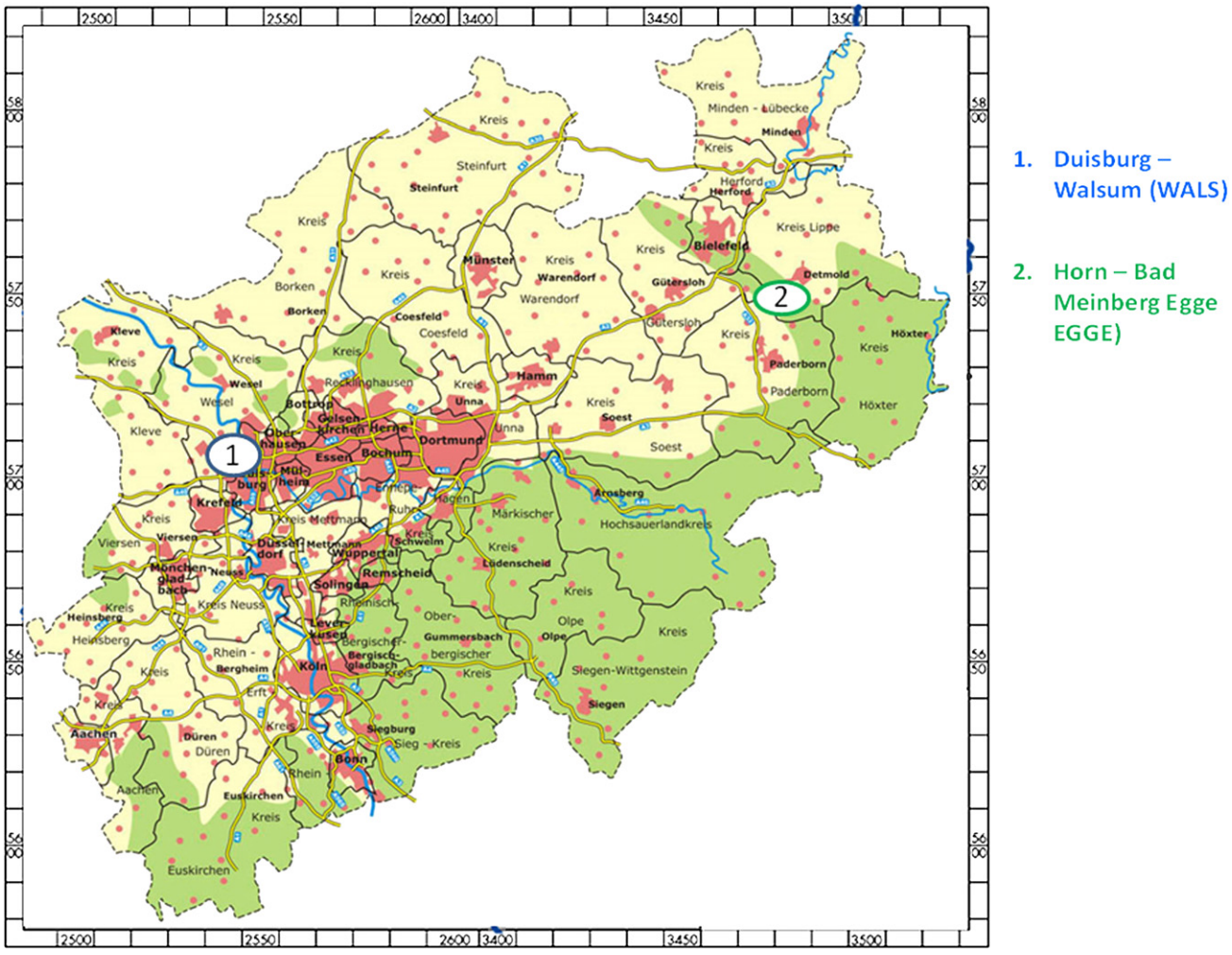

Fig. 1. Measurement stations in North Rhine – Westphalia; Source: wuppertal.de (2012).

not available). The measuring height at all of the stations was 3.5 m above ground level (agl). Wind speed and direction were measured at the height of 23 m agl. The detection limit was 0.3 m s^{-1}.

All of the data are half-hour means. Before starting the analysis, all of the data were checked for quality using box–whisker diagrams (Melkonyan, 2011).

The probability of the number of days when ozone will exceed its limit value in the future (in regard to the given maximum daily temperature) was calculated using both probability theory and the ARIMA model.

In the classical probability statement, the probability that event A will occur is the number of ways (frequency) that a specific event can occur (n) related to the total possible outcomes (N), as calculated using Formula (1) (Schefler, 1988).

$$P(A) = n/N \tag{1}$$

N was defined as the number of days with a maximum daily temperature over 25 °C (summer days), and n was the number of events when ozone exceeded its limit value according to the given maximum daily temperatures.

The Autoregression Integrated Moving Average (ARIMA (p,d,q)) model is a tool to analyse the character of autocorrelated time series, providing the opportunity to predict the factors' behaviour in the future (Grimmer, 2007). ARIMA can be fitted by least-squares regression, minimising the error terms, thus being a good practice to provide an acceptable fit to the data. With autocorrelation and partial autocorrelation analyses, the ARIMA model can be defined (specifically, the order of p, d and q), where p is the order of an autoregression (AR) model, d is the number of differentiation of the time series (if there is autocorrelation), and q is the order of moving average (MA) processes (Grimmer, 2007).

Most time series consist of elements that are serially dependent such that one can estimate a coefficient or a set of coefficients that describe consecutive elements of the series from specific, time-lagged elements, and therefore, each observation is made up of a linear combination of the previous elements (coefficient is ϕ which is between −1 and +1) and a random error component for the considered time period t (ε_t or random shock). An autoregression model of order p is denoted AR (p) and is described with Formula (2) (the term c is a constant):

$$Y_t = c + \sum_{i=1}^{p} \phi_i Y_{t-i} + \varepsilon_t \tag{2}$$

Disregarding the autoregression process, each element in the series can also be affected by the error of a past period (random shock) that cannot be accounted for by the autoregression components. Each observation is made up of a constant, linear combination of

prior random shock and random error components: the moving average process of the order q is denoted MA (q) and is described with Formula (3):

$$Y_t = \mu + \sum_{i=1}^{q} \theta_1 \varepsilon_{t-q} + \varepsilon_t \quad (3)$$

Combining these two models, we obtain an ARMA (p,q) model (Formula (4)).

$$Y_t = c + \mu + \sum_{i=1}^{p} \phi_i Y_{t-i} + \sum_{i=1}^{q} \theta_1 \varepsilon_{t-q} + \varepsilon_t \quad (4)$$

The ARIMA model was used to directly predict the number of days with ozone exceedance in the future up to the year 2020. The year 2020 was chosen because of the limited reliability of the model to predict for longer time periods. The model was also used to predict the maximum daily temperature for the same period of time. Using maximum daily temperature values until 2020 and with the probability of ozone exceedances for the given maximum daily temperature, the number of days when ozone would exceed its target value was estimated indirectly. Later, the directly and indirectly predicted ozone exceedances were compared to determine the reliability of both of the methods.

4. Results

4.1. Interrelations among ozone, its precursors and meteorological parameters

To predict ozone behaviour for the future, it is important to identify the variables on which ozone is merely dependent. First, a correlation matrix was calculated between the maximum ozone concentrations and the NO, NO_2, NO/NO_2 ratio, maximum air temperature, radiation, humidity, precipitation and wind speed values. Daily values were used (Tables 1a and b).

At both of the stations, the highest positive correlation coefficients were obtained between maximum ozone, maximum temperature and maximum radiation. For example, for WALS, the correlation coefficients between the maximum ozone and the maximum daily temperature and maximum radiation were 0.75 and 0.73, respectively. The latter might be explained by the photochemical production of ozone. The high correlation between ozone and temperature is a result of high correlation between maximum daily temperature and maximum radiation and the temperature dependence of BVOC emissions and PAN stability. The highest negative correlations existed between maximum ozone and relative humidity (−0.59). The latter is mainly explained by correlations between the relative humidity and the temperature (−0.49) and radiation (−0.67), (similar values were obtained by Meleux et al., 2007). The correlation of maximum ozone with precipitation, as well as with wind speed, was non-significant. The correlation between maximum ozone and NO concentration was better for WALS (−0.37) than for EGGE (−0.19) due to the influence of local emissions of NO. For the same reason, the correlation between maximum ozone and the NO/NO_2 ratio was better for WALS (−0.38) than for EGGE (0.07).

Table 1a
Correlation coefficients between maximum ozone and NO, NO_2, NO/NO_2 ratio, maximum temperature, maximum radiation, relative humidity, precipitation, wind speed; daily values at the industrial (WALS) and rural background (EGGE) stations (1984–2007).

Stations	WALS	EGGE
Correlation matrix	Max O_3	Max O_3
NO	−0.37	−0.19
NO_2	−0.21	−0.36
NO/NO_2	−0.38	0.07
Max temp.	0.75	0.65
Max rad.	0.73	0.68
Rel. hum.	−0.59	−0.64
Prec.	−0.04	−0.10
Wind speed	−0.14	−0.23

Table 1b
Correlation matrix of the given meteorological variables and ozone at the industrial station (WALS).

	Max O_3	Max temp.	Max rad.	Rel. hum.	Abs. hum.	Prec.	Wind speed
Max O_3	1						
Max temp.	0.75	1					
Max rad.	0.73	0.73	1				
Rel. hum.	−0.59	−0.49	−0.67	1			
Abs. hum.	0.56	0.87	0.46	−0.08	1		
Prec.	−0.04	−0.02	−0.17	0.30	0.14	1	
Wind speed	−0.14	−0.22	−0.27	0.02	−0.18	0.25	1

The given results show that the relationship between ozone and the NO/NO_2 ratio was less pronounced (−0.38) than the correlation between maximum ozone and maximum daily temperature (0.75). To filter out which variable (NO/NO_2 ratio or maximum daily temperature) had a greater influence on ozone formation, partial correlations were carried out excluding the NO/NO_2 ratio (Table 2a) and maximum daily temperature (Table 2b), respectively. The results of the partial correlation for WALS show that by excluding the NO/NO_2 ratio, the correlation coefficient between the maximum ozone and maximum daily temperature became slightly smaller (0.73) in comparison to Table 2b (0.75) (decrease by 2.7%). In contrast, by excluding the maximum daily temperature, the correlation between the maximum ozone concentration and the NO/NO_2 ratio fell deeply (−0.31) in comparison to the initial result (−0.38) (by 18.4%).

Therefore, it can be concluded that ozone dependency on temperature for a given level of NO_x concentration might be more relevant than the NO_x concentration itself because ozone chemistry is dependent on NO_x nonlinearly. Hence, the further analysis is concentrated on maximum ozone concentrations in dependence on maximum daily temperature.

4.2. Ozone concentrations and its target value

The number of days when ozone concentrations exceeded the target value (daily maximum 8-h average of 120 μg m^{-3}) was consolidated on an annual basis at the industrial (WALS) and at the

Table 2
Partial correlation coefficients among daily maximum ozone concentrations and daily mean NO, NO_2 concentrations, NO/NO_2 ratio and maximum temperature excluding (a) NO/NO_2 ratio and (b) excluding maximum temperature at the industrial station (WALS) (1984–2007); all values are 95% significant ($p < 0.05$).

(a)

Without NO/NO_2	Max O_3	NO	NO_2	Max temp
Max O_3	1	−0.05	−0.06	0.73
NO	−0.05	1	0.63	−0.07
NO_2	−0.06	0.63	1	−0.03
Max temp	0.73	−0.07	−0.03	1

(b)

Without max temp	Max O_3	NO	NO_2	NO/NO_2
Max O_3	1	−0.28	−0.17	−0.31
NO	−0.28	1	0.59	0.9
NO_2	−0.17	0.59	1	0.38
NO/NO_2	−0.31	0.9	0.38	1

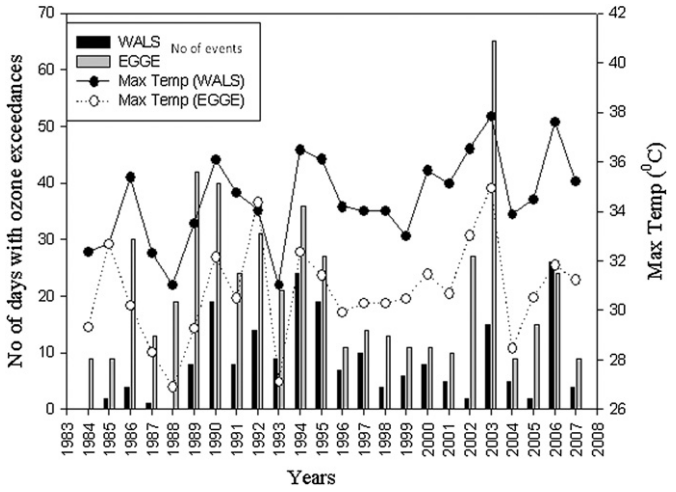

Fig. 2. Annual number of days when ozone exceeded its target value (maximum daily 8-h average of 120 μg m^{-3}) and maximum daily temperature at the industrial (WALS) and rural background (EGGE) stations (1984–2007).

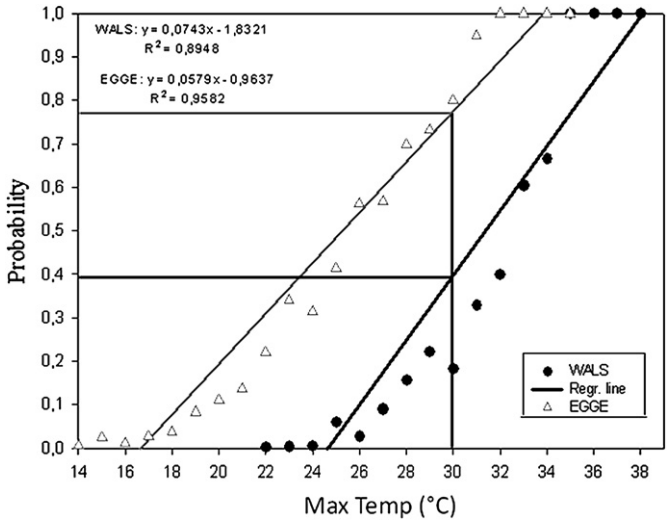

Fig. 3. Probability of ozone exceedances in regard to the given maximum temperature at the industrial (WALS) and the rural background (EGGE) stations (1984–2007).

rural background (EGGE) stations for the 1984–2007 period (Fig. 2). A slight, insignificantly increasing trend was observed together with an increasing maximum daily temperature at both of the stations.

The highly positive correlation between ozone and air temperature is reflected in assessing the probability of the number of days with ozone exceedances in regard to the given maximum daily temperature (Table 3). The number of days with a given maximum daily temperature was counted for each degree at the industrial (WALS) and rural background (EGGE) stations. Corresponding to the temperature, the number of days with ozone exceedances was counted. Because a probability is the ratio of occurred events to all of the possible cases, the probability that ozone exceeds its target value at a given maximum daily temperature was calculated by dividing the number of days when ozone exceeded its target value (at a given maximum daily temperature) to the number of events when corresponding maximum daily temperatures were registered.

In general, the maximum daily temperature was higher at the industrial station WALS, but ozone exceeded its target value at lower maximum daily temperatures (starting at 14 °C) and more frequently at the rural background station EGGE. For instance, only one day with ozone exceedance was observed at WALS at the maximum daily temperature of 22 °C (and there were 307 days with this maximum daily temperature at WALS); hence, probability is equal to 1/307 = 0.003. In contrast, at the rural background station (with only 186 days with this maximum daily temperature), 41 days with ozone exceedances were registered (the probability is equal to 41/186 = 0.22).

The probabilities of days with ozone exceedances depending on maximum daily temperature are also shown in Fig. 3. The regression line between the maximum daily temperature and the number

Table 3
Number of days with the given maximum temperature and ozone exceedances; the probability that ozone exceeds its target value for the given maximum temperature at the industrial (WALS) and rural background (EGGE) stations (1984–2007).

Max temp	No of days with max temp (WALS)	No of days with ozone exceed (WALS)	Probability (WALS)	No of days with max temp (EGGE)	No of days with ozone exceed (EGGE)	Probability (EGGE)
14				404	2	0.0050
15				339	8	0.0236
16				350	4	0.0114
17				329	9	0.0274
18				292	11	0.0377
19				279	23	0.0824
20				272	30	0.1103
21				234	32	0.1368
22	307	1	0.0033	186	41	0.2204
23	291	1	0.0034	156	53	0.3397
24	248	1	0.0040	143	45	0.3147
25	199	12	0.0603	121	50	0.4132
26	181	5	0.0276	89	50	0.5618
27	144	13	0.0903	81	46	0.5679
28	121	19	0.1570	53	37	0.6981
29	113	25	0.2212	41	30	0.7317
30	93	17	0.1828	15	12	0.8000
31	73	24	0.3288	20	19	0.9500
32	30	12	0.4000	9	9	1
33	43	26	0.6047	4	4	1
34	27	18	0.6667	2	2	1
35	13	13	1	1	1	1
36	4	4	1			
37	4	4	1			
38	3	3	1			

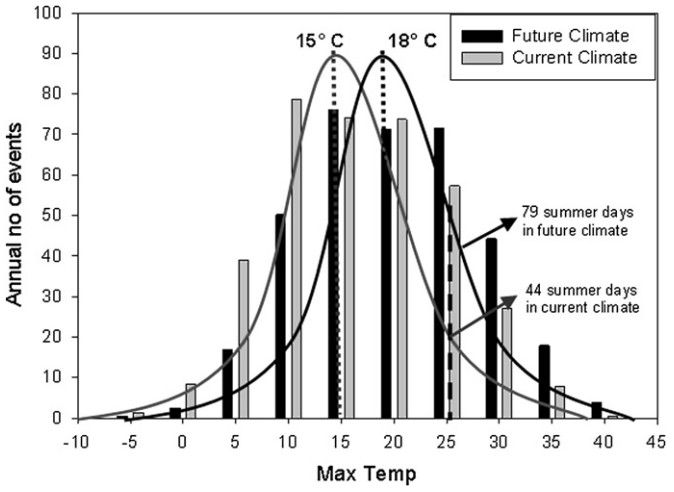

Fig. 4. Maximum daily temperature distribution at the industrial station WALS for the 1984–2007 period and in the future (2100), the black dashed line marks 25 °C (summer days).

of days with ozone exceedances at the rural background station EGGE is located above the regression line for the industrial station WALS. Thus, if we consider a maximum daily temperature of 30 °C, the probability that ozone exceeds its target value is approximately 0.4 at the industrial station WALS, whereas this probability is twice as high (0.77) at the rural background station EGGE. This result highlights the fact that ozone-forming potential is significantly higher in rural regions located relatively far away from the main sources of NO, which destroys ozone by reaction (R1), as well as higher levels of biogenic emissions.

4.3. Ozone projection in the future

4.3.1. Ozone projection until 2100 (probability theory)

Using the temperature increase of 3 K, the distribution curve of maximum daily temperature was synchronically shifted to the right by 3 K. Although using this method is a simplification of the future temperature projection, it can still be seen that temperature extremes in the future are likely to become more common.

An example is given for the industrial station WALS (Fig. 4). During the 1984–2007 period, the mean maximum daily temperature was 15 °C (a distribution fitting curve is represented as the grey line) and is suggested to be 18 °C in 2100 (the distribution fitting curve is represented as the black line in Fig. 4) at the industrial station WALS.

Integrating all of the days when the maximum daily temperature is higher than 25 °C (summer days), we see that the annual number of summer days of 44 in the current climate (1984–2007) will rise to 79 in the future (2100) (Fig. 4). In contrast to the industrial station WALS, the annual number of summer days at the rural background station EGGE in the current climate is only 17 and will be doubled (37 days) in the future, however, only to half of the number of days at the WALS station. The lower number of summer days at EGGE can be explained by the higher altitude above sea level and a lack of direct anthropogenic influence (with an annual mean of maximum daily temperature of only 10.8 °C observed at EGGE in the current climate).

Having shown the strong relations between the maximum daily temperature and ozone, the number of days was calculated when ozone exceeds its target value in the future climate based on the increased maximum daily temperature. The annual number of days with a maximum daily temperature of 22–38 °C was calculated (there was no event with ozone exceedances when the maximum daily temperature was below 22 °C for WALS, and a maximum daily temperature of 38 °C was the highest one registered during the 1984–2007 period). Then, this number of days was multiplied by the probability of ozone exceedances (Table 3) at the given maximum daily temperature not only for the current but also for the future climate (Table 4). These calculations were carried out for both the industrial (WALS) and rural background (EGGE) stations, but here, only WALS is given as an example.

The method using probability theory suggests that if temperature increases by 3 K by 2100, the number of days on which ozone will exceed its target value would sharply increase. At the industrial station WALS, there might be 19.3 days (8 days in the current climate), and at the rural background station EGGE, there might be 40.5 days (21 days in the current climate), which means that the number of days

Table 4
Annual number of days with the given maximum temperature (22–41 °C) and annual number of days when ozone exceeds its target value of maximum 8-h average of 120 μg m^{-3} for the current (1984–2007) and the future climates (2100) at the industrial station WALS.

Max temp	Annual number of days with the given max temp (current climate)	Annual number of days with the given max temp (future climate)	Probability that ozone exceeds its target value for the given max temp	Annual number of days when ozone exceeds its target value for the given max temp (current climate)	Annual number of days when ozone exceeds its target value for the given max temp (future climate)
22	12.7917	15.5833	0.0033	0.0417	0.0508
23	12.1250	14.0417	0.0034	0.0417	0.0483
24	10.3333	13.7500	0.0040	0.0417	0.0554
25	8.2917	12.7917	0.0603	0.5000	0.7714
26	7.5417	12.1250	0.0276	0.2083	0.3349
27	6.0000	10.3333	0.0903	0.5417	0.9329
28	5.0417	8.2917	0.1570	0.7917	1.3020
29	4.7083	7.5417	0.2212	1.0417	1.6685
30	3.8750	6.0000	0.1828	0.7083	1.0968
31	3.0417	5.0417	0.3288	1.0000	1.6575
32	1.2500	4.7083	0.4000	0.5000	1.8833
33	1.7917	3.8750	0.6047	1.0833	2.3430
34	1.1250	3.0417	0.6667	0.7500	2.0278
35	0.5417	1.2500	1	0.5417	1.2500
36	0.1667	1.7917	1	0.1667	1.7917
37	0.1667	1.1250	1	0.1667	1.1250
38	0.1250	0.5417	1	0.1250	0.5417
39	0.0000	0.1667	1	0.0000	0.1667
40	0.0000	0.1667	1	0.0000	0.1667
41	0.0000	0.1250	1	0.0000	0.1250

with likely ozone exceedance would increase by 135% at WALS and by 87% at EGGE. The relatively moderate increase at EGGE could be explained by the fact that days with higher maximum daily temperatures are more frequent at WALS than at EGGE.

The results of Table 4 are presented in Fig. 5a and b for the industrial (WALS) and rural background (EGGE) stations, respectively.

4.3.2. Ozone projection up to 2020 (ARIMA model)

The main aim was to compare the results of the indirect projection of ozone exceedances obtained by applying the probability theory and the direct projection of ozone exceedances using the ARIMA model. Because the reliability of the ARIMA model is constrained to shorter time periods, the target year 2020 was chosen. To prove the results obtained by the probability theory (excluding the possibility of coincidence), both the number of days with ozone exceedances and the maximum daily temperature were modelled using the ARIMA, and then the methodology, as given in this chapter, was applied by multiplying the probability of ozone exceedances for each degree by the frequency at which each temperature occurs.

The number of days when ozone would exceed its target value was calculated until the year 2020 with the help of the ARIMA model. To develop the ARIMA (p, d, q) model, first, the autocorrelation and the partial autocorrelation functions of the number of days with ozone exceedance were discussed. Accordingly, 2 autoregression (AR), and 0 moving average (MA) terms were used, differentiating the series only once. Thus, the ARIMA (2, 1, 0) model was developed for the industrial station WALS. The predicted number of days when ozone would exceed its target value is shown in Fig. 6. The results of the ARIMA (2, 1, 0) model show that on average, there would be 10.9 days on which ozone will exceed its target value at the industrial station WALS until 2020, which is 32% more than in the current climate (8.2 days during the 1984–2007 period).

To prove this result and also the probability of ozone exceedances based on maximum daily temperature, an ARIMA model was developed for the maximum daily temperature until 2020. With the help of autocorrelation and partial autocorrelation analysis, ARIMA (1, 1, 2) (1, 0, 0) was created. The results are shown in Fig. 7. The average maximum daily temperature rose to 15.77 °C at the industrial station WALS by 2020, which is 0.77 K higher than the 1984–2007 average. Using the same methodology of the frequency distribution curve of the maximum daily temperature and shifting

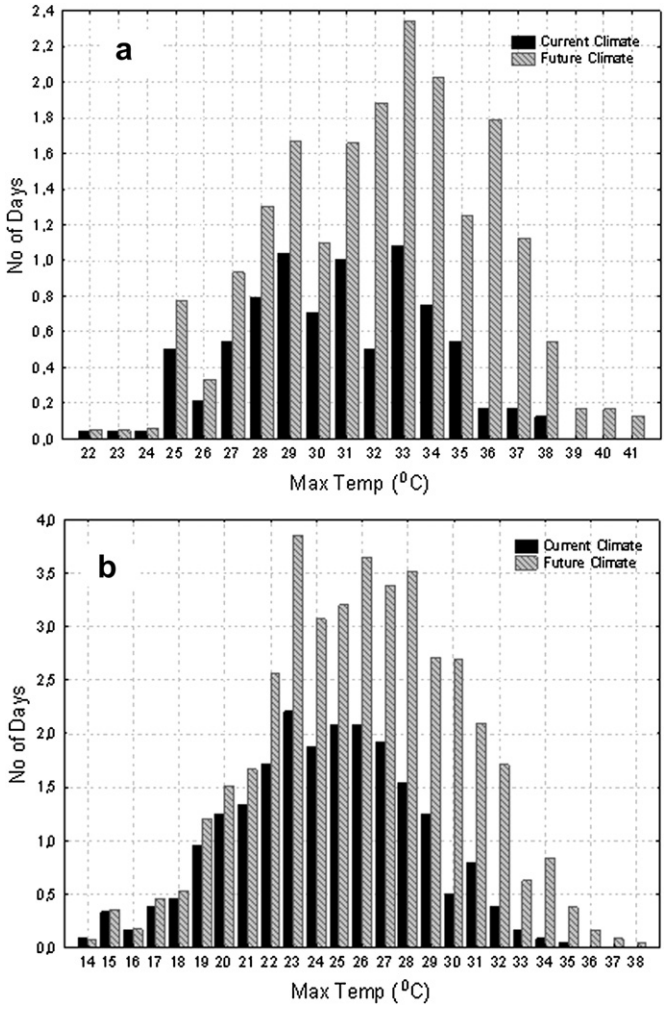

Fig. 5. Annual number of days when ozone exceeds its target value of maximum 8-h average of 120 μg m^{-3} for the current (1984–2007) and the future climates (2100) a) at the industrial (WALS) and b) at the background (EGGE) stations.

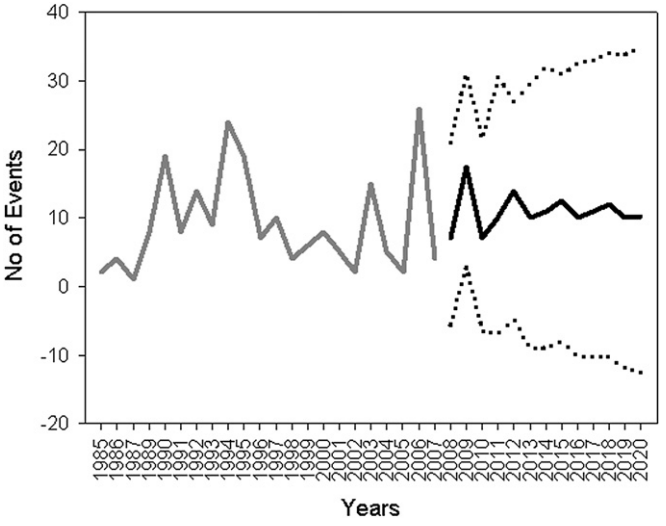

Fig. 6. Results of modelling the number of days with ozone exceedance until the year 2020 at the industrial station WALS using ARIMA (2, 1, 0) model; the black solid line indicates the observed data, grey solid line shows the results of the model and the black dashed line is the ±90% confidence interval.

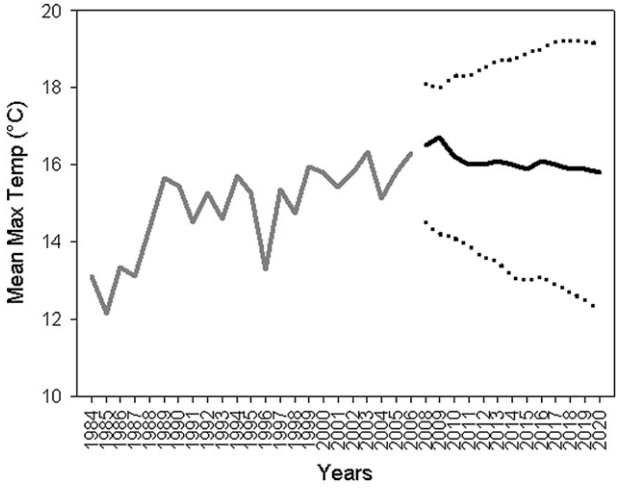

Fig. 7. Results of the maximum temperature forecast until the year 2020 at the industrial station WALS using the ARIMA (1, 1, 2) (1, 0, 0) model; the black solid line indicates the observed data, grey solid line shows the results of the model and the black dashed line is the ±90% confidence interval.

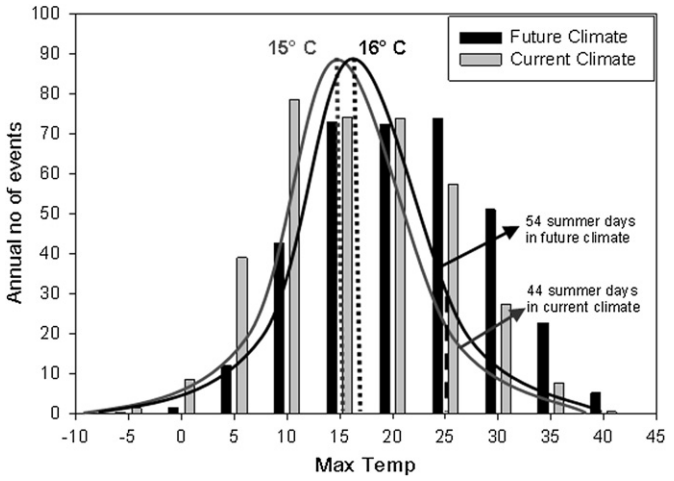

Fig. 8. Maximum temperature distribution at the industrial station WALS for the 1984–2007 period and in future (2020), black dashed line marks 25 °C (summer days).

it by 0.77 K to the right (Fig. 8), the frequency of a maximum daily temperature at each degree was obtained (Table 5, 1st column). As can be seen in Fig. 8, not only the average maximum daily temperature but also the number of summer days (maximum daily temperature $\geq$ 25 °C) increased by 22% to 54 days.

Using the probabilities of ozone exceedances for each degree of maximum daily temperature (given in Table 4), the annual number of days with ozone exceedance was 10.8 on average (Table 5). This result is in perfect accordance with the one obtained using the ARIMA (2, 1, 0) model (10.9 days). Hence, it can be concluded that both of the approaches produced reliable results.

The exact analysis of events with highozone concentrations allows the number of days when ozone exceeds its target value of a daily maximum 8-h average (120 μg m^{-3}) to be modelled. Both of the methods (probability analysis and the ARIMA model) showed that in the near future (until the year 2020) the number of these events would increase by 31% as a result of increased temperature (by 0.77 K on average) and by 135% until the year 2100 (if temperature increases by 3 K).

Table 5
Annual number of days with the given maximum temperature and ozone exceedance at the industrial station (WALS) in 2020 (based on results showed in Fig. 7 and probability of ozone exceedances in Table 4).

Max temp	Annual no of days with the given max temp in 2020	Probability of ozone exceedances	Annual no of days with ozone exceedances in 2020
22	14.7917	0.0033	0.0482
23	13.4167	0.0034	0.0461
24	11.7917	0.0040	0.0475
25	10.7083	0.0603	0.6457
26	8.2917	0.0276	0.2291
27	7.4583	0.0903	0.6733
28	6.0000	0.1570	0.9421
29	4.9167	0.2212	1.0878
30	5.2500	0.1828	0.9597
31	3.6667	0.3288	1.2055
32	2.6667	0.4000	1.0667
33	1.2500	0.6047	0.7558
34	1.8333	0.6667	1.2222
35	0.8750	1	0.8750
36	0.5833	1	0.5833
37	0.2083	1	0.2083
38	0.1667	1	0.1667
39	0.0417	1	0.0417
Mean no of days with ozone exceedances			10.8

5. Conclusions

This paper is devoted to ozone concentration analysis in regard to ozone precursors (here, only NO_x; VOC data were not available) as well as air temperature and its increase in the future climate as a consequence of global climate change (Schär et al., 2004; Meleux et al., 2007). Because ozone correlates with temperature (Lin et al., 2001; Solberg et al., 2005; Jacob and Winner, 2009), the projection of the number of days with ozone exceedances in the future climate (once for 2100 and 2020) were analysed by determining the exact interrelations between ozone concentrations and maximum daily temperature in the current climate (1984–2007). The results obtained using probability theory and the ARIMA model could be a very good start to project ozone in the future in more detail.

The sudden increases of ozone concentrations during the years 2003 and 2006 as a result of heat waves (Bruckmann et al., 2003a,b; Solberg et al., 2005; Meleux et al., 2007; Fouillet et al., 2008) were the motivation of this investigation. Based on the dependence of ozone concentrations on temperature, discovered from case studies of these heat waves, modelling ozone behaviour in the future climate is of great importance.

An ozone forecast for the future was conducted considering only maximum daily temperature, eliminating the influence of ozone precursors because the correlation between maximum ozone and maximum daily temperature was greater (0.75) than the correlation between ozone and NO (−0.37), NO_2 (−0.21) and the NO/NO_2 ratio (−0.38) for the industrial station WALS. Thus, emphasis was given to temperature in the ozone concentration forecast by fixing NO and NO_2 concentrations and varying only temperature.

However, not simply the ozone concentrations but also the number of days when ozone exceeded its target value (maximum 8-h average of 120 μg m^{-3}; the target value enforced since 2010 (LANUV NRW, 2010)) were analysed on an annual basis in regard to the maximum daily temperature.

By analysing the maximum daily temperature and the number of days on which ozone exceeded its target value at the industrial (WALS) and rural background (EGGE) stations, it could be stated that although the maximum daily temperature was higher at WALS, the number of days with ozone exceedance was higher at EGGE (21 days on annual basis) than at WALS (8 days on annual basis), and the frequency of ozone exceedances at the rural background station was higher than at the industrial one. This finding might be explained by a higher ozone-forming potential (due to higher emission rates of biogenic VOC) and less ozone degradation (due to lower concentrations of NO) at the rural background station. Because of these findings it must be noted that projections for one station cannot be transferred to any other stations.

After establishing clear relations between the maximum daily temperature and the number of days when ozone exceeded its target value, the next step was to predict the number of days with ozone exceedances for the future climate. For the year 2100, the IPCC A2 emission scenario was taken into account, according to which a temperature increase of 3 K is possible. Hence, the frequency distribution of each degree of temperature was calculated for the current climate (1984–2007), and the latter was shifted by 3 K to the right for the future climate (2100) (the same methodology was carried out by Schär et al., 2004). This shift means that the number of days when the maximum daily temperature is higher than 30 °C increased from 10 to 28. This result corresponds to the one obtained by Beniston (2004), predicting an increase of the number of hot days from 8 to 38 in Bazel, Switzerland.

According to the probability of ozone exceedances for each degree of temperature, the number of days on which ozone would exceed its target value in 2100 was calculated. Because there will be

19.5 ozone days at WALS and 40.5 days at EGGE, the number of high-ozone days will most likely rise by 87% at EGGE and by 135% at WALS. This result might be explained by the fact that higher maximum daily temperatures will be more frequent at the industrial station than at the rural background one, leading to shorter lifetimes of peroxyacetylnitrate (PAN) and other peroxyacylnitrates. Hence, emitted VOCs and NO_x from nearby sources at the WALS station cannot be stored and transported to rural areas as PAN but will start to produce ozone just after emission (Sillman and Samson, 1995; Beine et al., 1997).

A projection of the number of days with ozone exceedance was also carried out for the year 2020, when a forecast of the maximum daily temperature using the ARIMA model is realistic. The ARIMA (1, 1, 2) (1, 0, 0) model showed that the maximum daily temperature will increase on average by 15.77 °C in 2020, which is 0.77 K higher than in the current climate (1984–2007). By shifting the frequency of temperature distribution and using the probability of ozone exceedances for each degree of temperature, it can be seen that there will be 10.8 days with ozone exceedances. Nearly the same result (10.9) is obtained by calculating the number of days with ozone exceedance directly using the ARIMA (2, 1, 0) model. The estimation of 10.8 or 10.9 days with ozone exceedance at WALS in NRW is in good accordance with the results obtained by Forkel and Knoche (2006), who carried out simulations using the Meteorologie Chemie Modell (MCCM model) and calculated that there will be 3 and 13 high-ozone days in Northern and Southern Bavaria, respectively.

Acknowledgements

We express our gratitude to LANUV NRW (Environmental State Agency for Nature, Environment and Consumer Protection), especially to Dr. Ulrich Pfeffer and Dr. Reinhold Beier, for kindly providing the necessary data. We also thank DAAD (German Academic Exchange Service) for financing an academic PhD position in the framework of this project.

References

Atkinson, R., 2000. Atmospheric chemistry of VOCs and NOx. Atmospheric Environment 34, 2063–2101.
Barett, L.A., Bunce, N.J., Gillespie, T.J., 1998. Estimation of tropospheric ozone production using concentrations of hydrocarbons and NOx, and a comprehensive hydrocarbon reactivity parameter. Journal of Photochemistry and Photobiology A Chemistry 113, 1–8.
Beine, H.J., Jaffe, D.A., Herring, J.A., Kelley, J.A., Krognes, T., Stordal, F., 1997. High-latitude springtime photochemistry. Part I: NOx, PAN and ozone relationships. Journal of Atmospheric Chemistry 27, 127–153.
Beniston, M., 2004. The 2003 heat wave in Europe; a shape of things to come? An analysis based on Swiss climatological data and model simulations. Geophysical Research Letters 31, 1–4.
Booker, R., Muntifering, R., McGrath, M., Burkey, K., Decoteau, D., Fiscus, E., Manning, W., Krupa, S., Chappelka, A., Grantz, D., 2009. The ozone component of global change: potential effects on agricultural and horticultural plant yield, product quality and interactions with invasive species. Journal of Integrative Plant Biology 51, 337–351.
Bruckmann, P., Geiger, J., Hartmann, U., Wurzler, S., 2003a. Die Ozonepisode im Juli und August 2003. Landesumweltamt Bericht vom 22.08.03, pp. 1–15.
Carter, W.P.L., 1994. Development of ozone reactivity scales for volatile organic compounds. Journal of the Air and Waste Management Association 44, 881–899.
Costabile, F., Allegrini, I., 2007. Measurements and analysis of nitrogen oxides and ozone in the yard and on the roof of a street canyon in Suzhou. Atmospheric Environment 41, 6637–6647.
Derwent, R.G., Jenkin, M.E., Passant, N.R., 2007. Photochemical ozone creation potentials for different emission sources of VOCs under European conditions estimated with a Master Chemical Mechanism. Atmospheric Environment 41, 2570–2579.
Emeis, S., Schoenemeyer, T., Richter, K., Ruckdeschel, W., 1997. Sensitivity of ozone production to VOC and NOx emissions. A case study with the box-model BAYROZON. Meteorologische Zeitschrift 6, 60–72.
Forkel, R., Knoche, R., 2006. Regional Climate change and its impact on photooxidant concentrations in Southern Germany; Simulations with a coupled regional climate – chemistry model. Journal of Geophysical Research 111, 13. http://dx.doi.org/10.1029/2005JD006748.
Fouillet, A., Rey, G., Wagner, V., Laaidi, K., Empereur-Bissonnet, P., Le Tertre, A., Frayssinet, P., Bessemoulin, P., Laurent, F., De Crouy-Chanel, P., Jougla, E., Hémon, D., 2008. Has the impact of heat waves on mortality changed in France since the European heat wave of summer 2003? A study of the 2006 heat wave. International Journal of Epidemiology 37, 309–317.
Fuentes, J.D., Lerdau, M., Atkinson, R., Baldocchi, D., Botenheim, J.W., Ciccioli, P., Lamb, B., Geron, C., Gu, L., Guenther, A., Sharkey, T.D., Stockwell, W., 2000. Biogenic hydrocarbons in the atmospheric boundary layer: a review. Bulletin of American Meteorological Society, 1537–1575.
Guenther, A., Geron, C., Pierce, T., Lamb, B., Harley, P., Fall, R., 2000. Natural emissions of non-methane volatile organic compounds, carbon monoxide and oxides of nitrogen from North America. Atmospheric Environment 34, 2205–2230.
Handisides, G.M., Plass-Dülmer, C., Gilge, S., Bingemer, H., Berresheim, H., 2003. Hohenpeissenberg Photochemical Experiment (HOPE 2000): measurements and photostationary state calculations of OH and peroxy radicals. Atmospheric Chemistry Physics 3, 1565–1588.
Jacob, D., Winner, D., 2009. Effect of climate change on air quality. Atmospheric Environment 43, 51–63.
Kuttler, W., 2011. Klimawandel im urbanen Bereich, Teil 1, Wirkungen (Climate change in urban areas, Part 1, Effects). Environmental Sciences Europe.
Lee, B.-S., Wang, J.-L., 2006. Concentration variation of isoprene and its implications for peak ozone concentration. Atmospheric Environment 40, 5486–5495.
Lin, C., Jacob, D., Fiore, A., 2001. Trends in exceedances of the ozone air quality standard in the continental United States, 1980–1998. Atmospheric Environment 35, 3217–3228.
Meleux, F., Solmon, F., Giorgi, F., 2007. Increase in summer European ozone amounts due to climate change. Atmospheric Environment 41, 7577–7587.
Melkonyan, A., 2011. Statistical analysis of long-term air pollution data in North Rhine – Westphalia, Germany. Westarp – Wissenschaften (Essener Ökologische Schriften 30).
Monks, P.S., 2004. Gas-phase radical chemistry in the troposphere. Chemical Society Reviews.
Mücke, H.G., Klasen, J., Schmoll, O., Szewzyk, R., 2009. Gesundheitliche Anpassung an den Klimawandel. Umweltbundesamt Pressestelle.
Narumi, D., Kondo, A., Shimoda, Y., 2009. The effect of the increase in urban temperature on the concentration of photochemical oxidants. Atmospheric Environment 43, 2348–2359.
Sadanaga, Y., Yoshino, A., Kato, S., Kajii, Y., 2005. Measurements of OH reactivity and photochemical ozone production in the urban atmosphere. Environmental Science and Technology 39, 8847–8852.
Saito, S., Nagao, I., Kanzawa, H., 2009. Characteristics of ambient C2–C11 non-methane hydrocarbons in metropolitan Nagoya, Japan. Atmospheric Environment 43, 4384–4395.
Schär, C., Vidale, P., Lüthi, D., Frei, C., Häberli, C., Liniger, M.A., Appenzeller, C., 2004. The role of increasing temperature variability in European summer heatwaves. Nature 427, 332–336.
Schefler, W., 1988. Statistics, Concepts and Applications. The Benjamin/Cummings Publishing Company, Inc..
Sillman, S., Samson, P., 1995. Impact of temperature on oxidant photochemistry in urban, polluted rural and remote environments. Journal of Geophysical Research 100, 497–508.
Sillman, S., 1999. The relation between ozone, NOx and hydrocarbons in urban and polluted rural environments. Millenial Review series. Atmospheric Environment 33 (12), 1821–1845.
Sillman, S., 2003. Tropospheric Ozone, and Photochemical Smog; Treatise on Geochemistry. Environmental Geochemistry, vol. 9. Elsevier (chapter 11).
Solberg, S., Coddeville, P., Forster, C., Hov, Ø., Orsolini, Y., Uhse, K., 2005. European surface ozone in the extreme summer 2003. Atmospheric Chemistry and Physics 5, 9003–9038.
Yoshino, A., Nakashima, Y., Miyazaki, K., Kato, S., Suthawaree, J., Shimo, N., Matsunaga, S., Chatani, S., Apel, E., Greenberg, J., Guenther, A., Ueno, H., Sasaki, H., Hoshi, J., Yokota, H., Ishii, K., Kajii, Y., 2012. Air quality diagnosis from comprehensive observations of total OH reactivity and reactive trace species in urban central Tokyo. Atmospheric Environment 49, 51–59.

Internet-addresses

Bezirksregierung Düsseldorf, May, 2010. http://www.brd.nrw.de/index.jsp.
Bruckmann, P., et al., 2003b. Die Ozonepisode im Juli und August 2003, Landesumweltamt NRW: http://www.lua.nrw.de/luft/immissionen/aktluftqual/eu_o3_akt.htm.
Grimmer, J., 2007. Arima: Arima models for time series data. http://gking.harvard.edu/zelig.